Impact of climate and land-use changes on the water and sediment dynamics of the Tokoro River Basin, Japan

Muto, Yuka
Department of Civil Engineering, University of Tokyo

Noda, Keigo
Faculty of Applied Biological Sciences, Gifu University

Maruya, Yasuyuki
Graduate School of Engineering, Kyushu University

Chibana, Takeyoshi
Department of Civil Engineering, University of Tokyo

他

出版情報：Environmental Advances. 7, pp.100153-, 2022-04. Elsevier
バージョン：

Environmental Advances 7 (2022) 100153

Contents lists available at ScienceDirect

Environmental Advances

journal homepage: www.sciencedirect.com/journal/environmental-advances

Impact of climate and land-use changes on the water and sediment dynamics of the Tokoro River Basin, Japan

Yuka Muto [a,*], Keigo Noda [b], Yasuyuki Maruya [c], Takeyoshi Chibana [a], Satoshi Watanabe [d,*]

[a] Department of Civil Engineering, University of Tokyo, 7-3-1 Hongo, Bunkyo-ku, Tokyo 113-8656, Japan
[b] Faculty of Applied Biological Sciences, Gifu University, 1-1 Yanagido, Gifu 501-1193, Japan
[c] Graduate School of Engineering, Kyushu University, 744 Motooka, Nishi-ku, Fukuoka 819-0935, Japan
[d] Disaster Prevention Research Institute, Kyoto University, Gokasho, Uji, Kyoto 611-0011, Japan

1. Introduction

Water and sediment dynamics considerably influence the ecology, water utilization, and human activities within river basins. Therefore, it is critical to evaluate future changes in these dynamics.

Previous studies have analyzed the impact of climate change (Kalogeropoulos and Chalkias 2013; Luo et al., 2013;Meng et al., 2016; Milly et al., 2005; Mourato et al., 2015; Zabaleta et al., 2014) and land-use/cover changes (Kalantari et al., 2014; Noda et al., 2017; Pinokius et al., 2003), as they are considered the two key drivers exerting influence on water and sediment dynamics. The combined effects of climate and land-use/cover changes have also been analyzed (e.g., Li et al., 2009; Zhang et al., 2012), which have revealed that the impact of climate change can either be accelerated or restrained by land-use changes.

The effects of future land-use/cover changes were analyzed using land-use/cover scenarios based on the socio-economic conditions of each watershed. The major scenarios considered include the expansion of agricultural fields (Azimi Sardari et al., 2019; Molina-Navarro et al., 2014), changes in forest areas (Begueria et al., 2003; Khoi and Suetsugi, 2014; Li et al., 2012; Lopez-Moreno et al., 2014; Mango et al., 2011; Montenegro and Ragab, 2012; Shao et al., 2018), urbanization (Wilson and Weng, 2011), and changes in crop types within agricultural fields (Carvalho-Santos et al., 2015; Montenegro and Ragab, 2012; Serpa et al., 2015).

Other authors, such as Walling (2006) and Noda et al. (2019), assessed sediment dynamics resulting from social development and economic growth, using long-term historical data. Walling (2006) examined rivers in large continents and concluded that, except for reservoirs that caused sediment entrapment, other activities related to the development of human society and economy, i.e., land clearance for agricultural and other activities contributing to land disturbances such as logging and mining, have led to an increase in sediment transport. Conversely, Noda et al. (2019) examined sediment transport on an island in the Republic of Palau and suggested that long-term sediment transport trends in this area were inconsistent with the conclusions reported by Walling (2006). This was attributed to the specificity of small islands; as they were highly dependent on resources outside the islands, they could reduce the use of land resources within the islands. Additionally, the major industry in the region was nature-based tourism, which promotes the improvement of sustainable land resource use.

In addition to the perspectives provided by the former studies, it is imperative to investigate how climate change and land-use change induced by depopulation, influence the water and sediment dynamics. Japan is currently experiencing rapid depopulation, particularly in rural areas (NIPSSR, 2018). The human impact on water and sediment dynamics is assumed to be similar to what was reported by Walling (2006) for most river basins in Japan. However, as depopulation is a new transition in human society, the effects on water and sediment dynamics derived from reductions in agricultural and urban areas, have not been analyzed thus far; which is important for areas in which depopulation is currently occurring or projected to occur.

This study aimed to investigate the independent and combined effects of climate and land-use/cover changes on water and sediment dynamics in the Tokoro River Basin, where the occurrence of both significant climate change and depopulation has been anticipated.

This study was conducted in five steps (Fig. 1):

(1) Calibration and validation of the Soil Water Assessment Tool (SWAT) for the Tokoro River Basin.
(2) Verification of the reproducibility of the discharge and suspended sediment (SS) loads calculated by SWAT, using the ensemble climate datasets obtained from the Japan Meteorological Agency Global Warming Projection Volume 9 (JMA-GWP9) (JMA; Japan Meteorological Agency, 2017).

* Corresponding authors.
E-mail addresses: muto@hydra.t.u-tokyo.ac.jp (Y. Muto), watanabe.satoshi.6t@kyoto-u.ac.jp (S. Watanabe).

https://doi.org/10.1016/j.envadv.2021.100153
Received 2 June 2021; Received in revised form 12 December 2021; Accepted 13 December 2021
Available online 16 December 2021

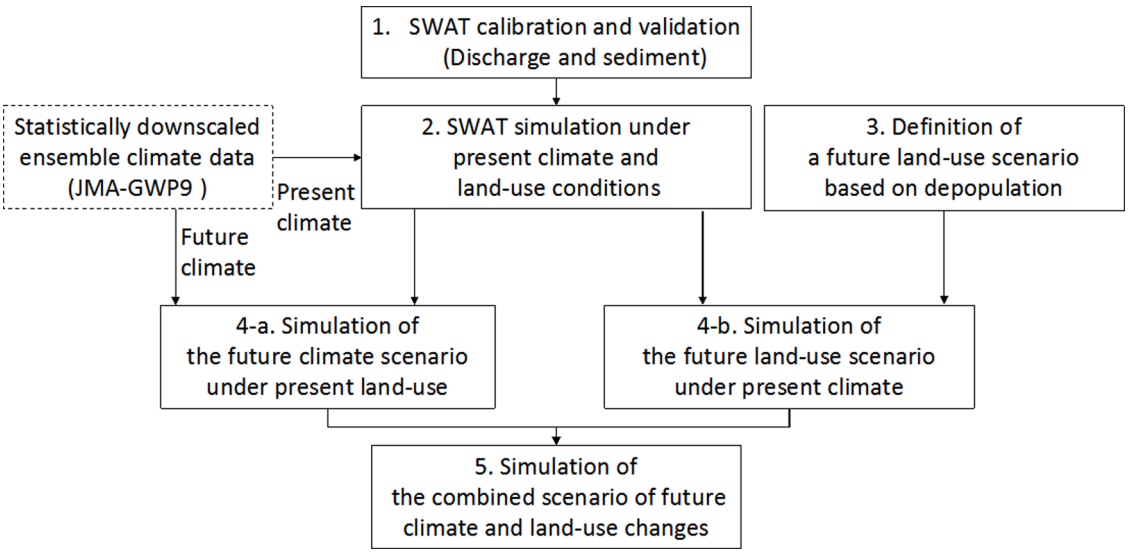

Fig. 1. Workflow of this study.

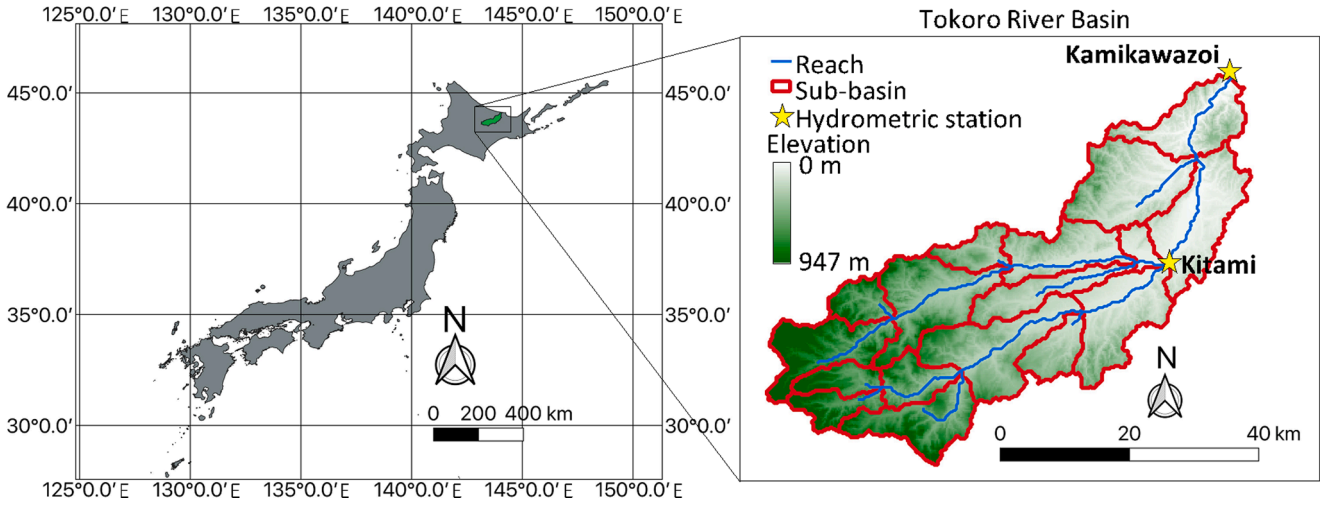

Fig. 2. Location, hydrological network, sub-basins, hydrometric stations and elevation map of the Tokoro River Basin.

(3) Definition of a future land-use scenario based on a depopulation trend.
(4) Simulation of the individual effects of future climate and land-use changes on discharge and SS loads.
(5) Simulation of the combined impacts of future climate and land-use changes on discharge and SS loads.

2. Methodology

2.1. Study area

The target area of this study was the Tokoro River Basin, a region located in northern Japan. The Tokoro River originates in Mount Mikuni (altitude 1541 m) and runs to the Sea of Okhotsk (Fig. 2), with a drainage area of 1930 km^2. At the Kamikawazoi hydrometric station (Fig. 2), the average annual temperature for the period 1978–2004 was 5.8 °C, with the average annual minimum and maximum temperatures being –24.2 °C and 32.7 °C, respectively (MLIT, 2006). At the same location, the annual average precipitation for the same period was 726.8 mm (MLIT, 2006). The rainy season occurs in summer, and a substantial proportion of precipitation occurs as snowfall in winter.

The water quality in the target area has historically remained a concern. Since the 1980s, water quality indices such as the biochemical oxygen demand and total nitrogen and phosphorus concentrations have been rated as high (LCCSRTRB, 2009). Additionally, river discharge during the summer has been insufficient in certain years. At the Kitami hydrometric station (Fig. 2), the river discharge during the summer season fell below the “normal discharge” (approximately 8 m^3/s) in four years from 1993 to 2002 (LCCSRTRB, 2009). The “normal discharge” is defined by the Ministry of Land, Infrastructure and Transport (MLIT) as the total amount of discharge necessary to maintain the riverine ecosystem and to ensure water resource provision.

Considering the major industries within the basin, sustainable water resource management is critical. One of the main industries in the Tokoro River Basin is agriculture, and crops such as onions and sugar beets are intensively cultivated. Another important industry in the downstream areas is aquaculture, which includes the farming of scallops, salmon, and trout. The maintenance of river discharge is essential for agricultural activities and for ensuring water quality in coastal areas. Among the water quality parameters, sediment concentration is one of the most important indicators in the Tokoro River Basin because high sediment concentrations have caused the death of scallops and the interruption of water supply (Ishida et al., 2010).

The Tokoro River Basin is predicted to undergo significant climate

Table 1
Historical and estimated future population in the municipalities within the Tokoro River Basin.

Year	1925	2010	2045	2060
Kitami City	27,396	125,689	82,362	62,890
Kunneppu Town	6070	5435	2759	1865
Oketo Town	7940	3428	1364	–
Total	41,406	134,552	86,485	–

Table 2
Calibrated SWAT parameters.

	Parameter name	Description	Optimizing method	Calibrated value
Discharge parameters	ALPHA_BF	Baseflow alpha factor	Replace	0.53
	GWQMN	Threshold water depth in the shallow aquifer for flow	Replace	3602.19
	GW_REVAP	Groundwater 'revap' coefficient	Replace	0.19
	SOL_K	Saturated hydraulic conductivity	Relative	92%
	CH_K2	Channel effective hydraulic conductivity	Replace	382.27
	CH_N2	Manning's value for main channel	Replace	0.01
Discharge parameters (related to snow)	SMTMP	Snowmelt base temperature	Replace	3.07
	SFTMP	Snowfall temperature (°C)	Replace	1.47
	SMFMX	Melt factor for snow on 21 June (mm H2O°C−1 d−1)	Replace	8.91
	SNOCOVMX	Minimum snow water content that corresponds to 100% snow cover	Replace	241.84
Sediment parameters	SPEXP	Channel re-entrained exponent parameter	Replace	1.01
	SPCON	Channel re-entrained linear parameter	Replace	0.00
	PRF	Sediment routing factor in main channels	Replace	1.16
	CH_EROD	Channel erodability factor	Replace	0.38
	CH_COV	Channel cover factor	Replace	0.14
	USLE_P	Support practice factor	Replace	0.14
	USLE_K	Soil erodability factor	Relative	89%

changes in the future. The Ministry of Education, Culture, Sports, Science and Technology (MECSST) and the Japan Meteorological Agency (JMA) (2020) have concluded that the temperature will increase more on the Pacific Ocean side of northern Japan, where the basin is located, compared to other parts of the country. No statistically significant change was predicted for the annual and seasonal precipitation amounts. However, the considerable amount of snow in this area during winter has been assumed to decrease by approximately 60% in the Representative Concentration Pathway 8.5 (RCP8.5) scenario in the late 21st century (2076–2095) compared to the late 20th century (1980–1999).

In addition to future climate changes, the population in the basin is foreseen to decrease significantly in the near future compared to other areas in Japan. Table 1 shows that the total population of the three municipalities (Kitami City, Kunneppu Town, and Oketo Town) in the Tokoro River Basin in 2010 was 134,522. According to the National Institute of Population and Social Security Research (NIPSSR) (2018), the population is estimated to decrease by 33% by 2045. It is also assumed that the population in this area will continue to decrease, as the proportion of elderly people is estimated to increase. The population estimates for 2060 for all municipalities, except for Oketo Town, confirm this trend (Kitami city 2020; Kunneppu City, 2020).

2.2. Hydrological modeling

2.2.1. SWAT setup

This study used the SWAT model, a semi-distributed hydrologic model that could be used to analyze the effects of climate or land-use changes on water balance, sediment transport, and water quality by altering weather and land-use input data. Outputs are calculated daily; therefore, the model is suitable for analyzing long-term trends in water and sediment dynamics as is the case in this study, as opposed to runoff processes during flood events (Neitsch et al., 2009).

SWAT divides a watershed into sub-basins based on topography and river networks and further divides these sub-basins into hydrologic response units (HRUs) based on the soil, slope, and land-use characteristics. Within each HRU, the daily water balance and soil erosion are calculated, summed at the sub-basin level, and are finally distributed to the outlet of the watershed. In SWAT, surface runoff is calculated using the Soil Conservation Service Curve Number method (SCS, 1985). Soil erosion is calculated using the modified universal soil loss equation (Williams, 1975). In the present work, the SWAT physics-based approach was adopted for simulating channel erosion, using the simplified Bagnold stream power model (Neitsch et al., 2009). According to this approach, erosion is defined by the critical and actual shear stress at the riverbank and riverbed, within the range of the sediment transport capacity described by Bagnold (1977). For the present study, the QSWAT version 1.9 was used.

A watershed covering most of the Tokoro River Basin and its sub-basins was delineated using a digital elevation model (DEM) and river network data (MLIT, 2021a). The DEM used in this study was based on that published by the Geospatial Information Authority of Japan –GIAJ (2021). The DEM was upscaled to a resolution of approximately 200 m, using the inverse distance weighted method (Watson and Philip, 1985) in ArcGIS. The outlet of this watershed was situated at Kamikawazoi, which is the most downstream observation point of river discharge and water quality in the basin (Fig. 2). The watershed was divided into 17 sub-basins (Fig. 2). Additionally, HRUs for the baseline land-use scenario were created with the thresholds of soil, slope, and land-use set to 10%. The number of HRUs in the baseline scenario was 118. The distributions of slope classes and soil types are depicted in Fig. S1.

Daily precipitation and temperature data from six meteorological stations covering the watershed were used as input data for the model. Precipitation and temperature at these stations were measured by the Automated Meteorological Data Acquisition System –AMeDAS, developed by the JMA. The humidity, wind speed and solar radiation were simulated using the weather generator inbuilt in SWAT.

2.2.2. Model calibration, validation, and performance evaluation

The SUFI-2 algorithm from the SWAT calibration and uncertainty interface (Abbaspour 2015) was used in the present study. The advantages of using the SUFI-2 algorithm compared to other calibration methods are related to model performance, model prediction uncertainty, and model computational efficiency, which have been addressed in previous studies (Khoi and Thom, 2015; (Khoi et al., 2017)). The initial parameters selected for calibration were those related to discharge or soil erosion, and were not different for each land-use type (Table 2). As the target area has been reported to receive snowfall in

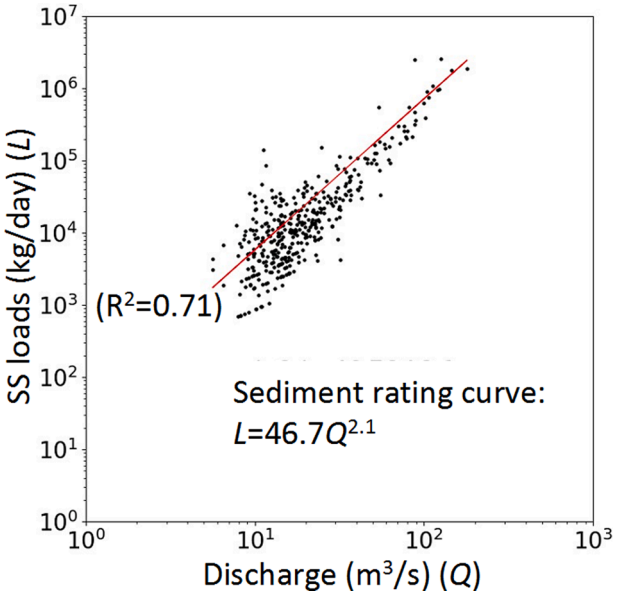

Fig. 3. Relationship between the observed daily SS loads (L) and observed daily discharge (Q) at the Kamikawazoi hydrometric station.

Table 3
Correspondence between MLIT and SWAT land-use classification.

MLIT classes	SWAT classes	SWAT_CODE
Rice paddy	Rice	RICE
Other agricultural land	Agricultural Land-Generic	AGRL
Forest	Mixed Forest	FRST
Wasteland	Barren or Sparsely vegetated	BSVG
Urban area	Urban High Density	URHD
Road	Urban Transportation	UTRN
Railway	Urban Transportation	UTRN
Others	Urban High Density	URHD
River and lake	Water	WATR
Beach	Water	WATR
Ocean	Water	WATR
Golf course	Pasture / Hay	PAST

winter, parameters related to snowfall or snowmelt were included, as was done by Tuo et al. (2018).

The observed discharge and SS concentrations data were obtained from the Japan Water Information System (MLIT, 2021b). There are four hydrometric stations in the Tokoro River Basin that measure both discharge and SS concentrations. To evaluate the changes in water and sediment regimes for the entire watershed, calibration and validation were conducted solely for the Kamikawazoi hydrometric station, which is the most downstream station of the watershed (Fig. 2). Data from 1983 to 1997 were used for model calibration, whereas data from 1998 to 2012 were used for model validation.

At the Kamikawazoi hydrometric station, discharge was measured daily, while SS concentrations were measured only once or twice a month. SS concentrations were determined using the method described by MLIT (2009). First, the sample was processed through a sieve with a mesh size of 2 mm to remove large particles such as leaves or plastics. Then, the sample was passed through a filter with a diameter of approximately 1 μm. The materials captured by the filter were then dried at 105–110°C until constant weight. Finally, SS concentrations were calculated by dividing the weight of the dried materials by the mass of the total sample.

The observed daily SS loads were calculated by multiplying the measured SS concentrations by the measured discharge. As SS concentrations were measured only once or twice a month, daily SS loads were estimated by interpolation. A sediment rating curve ($L = aQ^b$) was defined using the observed daily SS loads (L) and daily discharge (Q) ($R^2 = 0.71$) (Fig. 3). This curve was applied whenever SS concentrations were not measured, to estimate daily SS loads.

Calibration was carried out in two steps; first, parameters related to discharge were calibrated (Table 2), followed by those associated with sediment (Table 2). Five hundred iterations were repeated six and nine times respectively in the first and second steps of the calibration, to maximize the Nash-Sutcliffe efficiency (NSE) indicator (Nash and Sutcliffe, 1970). The parameter ranges were altered to a 95% confidence interval of the best solution at the end of every 500 iterations. Parameters were generated using the Latin hypercube sampling within the defined parameter ranges. For parameters whose values differed by soil type, the parameter ranges were set by considering the change in the percentage relative to the initial value (the "Relative" optimization method), to maintain the differences in values between soil types. For the other parameters, the ranges were simply replaced by the optimized values (the "Replace" optimization method). The optimization methods and calibrated values for each parameter are listed in Table 2.

Through the calibration process, a sensitivity analysis was conducted at every 500 iterations using the SUFI-2 algorithm (Abbaspour 2015). In this sensitivity analysis, 500 combinations of parameters were regressed against the NSE values. Then, the coefficient of each parameter was divided by its standard error (t-stat). All parameters presenting an absolute t-stat value below 1, for more than two times, were excluded. The remaining parameters were selected for calibration (Table 2).

Model performance was evaluated using three statistical indicators, as suggested by Moriasi et al. (2007): the NSE, the ratio of the root mean square error to the standard deviation –RSR (Singh et al., 2004), and the percent of bias –PBIAS (Gupta et al., 1999). The optimum value for NSE is 1, indicating very good model performance. For RSR, values should ideally be close to 0. Absolute PBIAS values close to 0 are indicative of good model performance. Negative PBIAS values are indicative of model overestimation, whereas positive values indicate model underestimation.

The reproducibility of model outputs was evaluated after model calibration and validation, using historical climate ensemble data. This process was necessary to confirm that the discharge and SS loads were properly simulated by the model when climate ensemble data were used instead of in situ weather observations, since climate change impacts were evaluated using historical and future climate ensemble data. The details of the climate ensemble data used in this study are provided in Section 2.3. The average annual discharge and SS loads simulated by the model were compared with the observed discharge and SS loads measured from 1983 to 2012, using the non-parametric Mann–Whitney U test (Mann and Whitney, 1947). The same test was performed for comparing the model outputs when using historical climate ensemble data with those using in situ weather observations.

2.3. Climate change scenario

Ensemble climate data for historical and future climate scenarios from the JMA-GWP9 (JMA; Japan Meteorological Agency, 2017) were used in the present study. The simulations were initially conducted using the global atmospheric model (GCM) MRI-AGCM3.2S (Mizuta et al. 2012) with a grid size of 20 km. Then, the results of the GCM were used as boundary conditions for the non-hydrostatic regional climate model (NHRCM05) (Sasaki et al., 2011), using a grid size of 5 km. Historical climate data from 1981 to 1999 were considered as the baseline scenario for this study. Future climate data from 2077 to 2095 under RCP8.5 scenario, with four different sea surface temperature warming patterns (ΔSSTs), were used as the worst-case scenario of climate change.

As climate simulations have some bias, they were corrected according to the observed dataset. Bias correction of precipitation data was conducted using the moving-window technique proposed by Watanabe et al., 2020, whereas temperature data were adjusted to the elevation of each meteorological station covering the Tokoro River

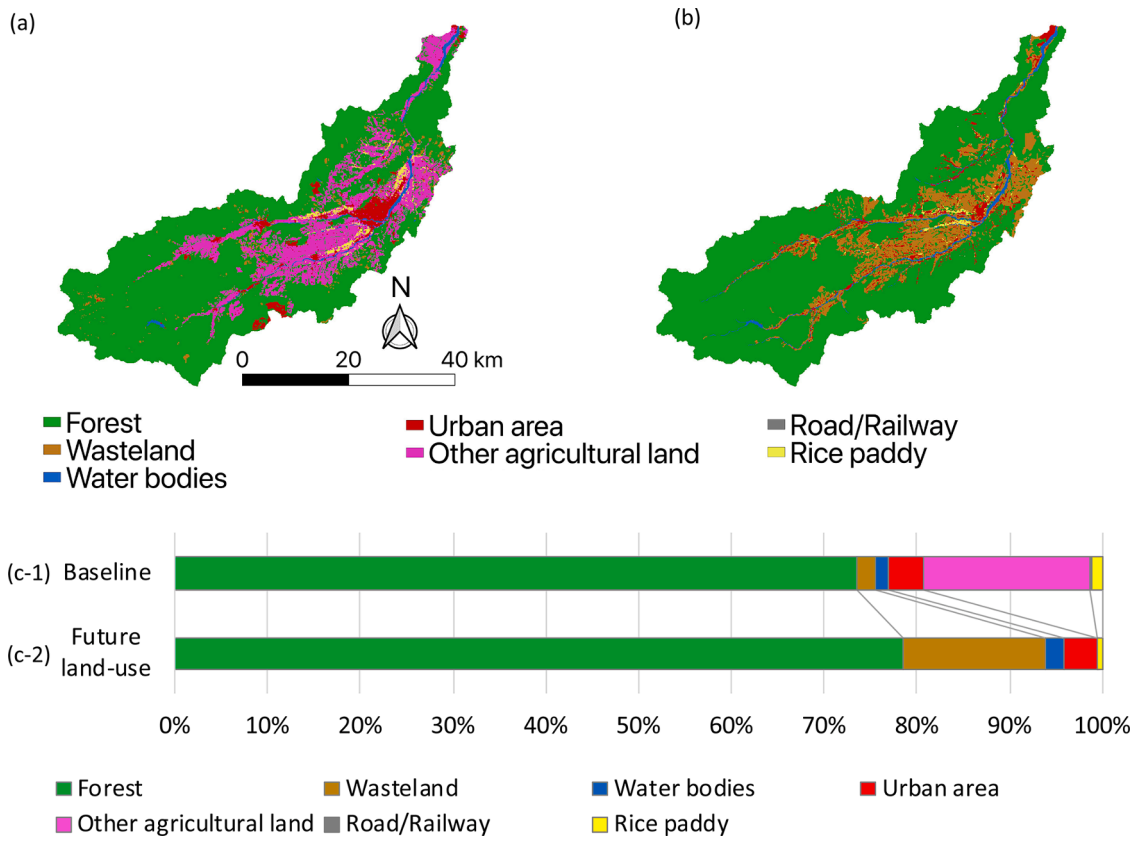

Fig. 4. Land-use map for the baseline (a) and future land-use scenario (b), and percentage of basin area occupied by each land-use type in the baseline (c-1) and future land-use scenario (c-2). All agricultural lands except for rice paddies are included in the classification "Other agricultural land." The major crops that are cultivated in these fields are onions and sugar beets.

Table 4
Number of agricultural workers and total agricultural area in the municipalities within the Tokoro River Basin.

	Number of agricultural workers			Total area of agricultural fields		
	2010	2015	Rate of change (2010–2015) (%)	2010 (km^2)	2015 (km^2)	Rate of change (2010–2015) (%)
Kitami City	3059	2498	18.3	170	162	4.7
Kunneppu Town	1133	1017	10.2	54	54	1.4
Oketo Town	401	370	7.7	37	35	3.2
Total	4593	3885	15.4	260	252	3.2

Basin.

2.4. Land-use change scenario

The baseline (present) land-use scenario was created using land-use mesh data with a grid size of 100 m, which was released by the MLIT (2021c). The land-use classification from MLIT was re-defined according to the classification used in SWAT (Table 3).

As explained in Section 2.1, depopulation is ongoing and is projected to continue in the target area. As in 1924, the total population of the municipalities within the Tokoro River Basin was 67% lower than that in 2010 (Table 1) (SB and MIAC, 2021), we have used historical land-use data from 1924 to define the future scenario of depopulation.

The digital map for the future land-use scenario was constructed based on an old land-use map from 1924. The old land-use map of 1924 was georeferenced and converted to be used in a geographic information system. The land-use shape file from 1924 was manually produced based on the map symbols drawn on the old map. Then, it was converted into mesh data with a grid size of 100 m. As the Kanoko Dam was constructed upstream the Tokoro River in 1983, the lake formed by the dam had to be incorporated into the future land use map since it was not present in 1924, but is likely to continue to exist in the future.

The baseline and future land-use scenarios of the Tokoro River Basin are depicted in Fig. 4. In the baseline land-use scenario, the plains were mostly occupied by agricultural fields. There were some areas with a high concentration of urbanized areas, such as the merging point of the two large river branches. In the future land-use scenario, the rice paddies, agricultural fields, and urbanized areas were reduced by 49.2%, 99.9% and 7.3%, respectively, because of the foreseen population decrease compared to the baseline scenario. Most of these areas were converted into forests or wastelands.

When defining the future land-use scenario, it was important to determine the extent to which this scenario reflects the reduction in agricultural areas due to depopulation. According to the census conducted by the Ministry of Agriculture, Forestry and Fisheries –MAFF in 2010 and 2015 (MAFF, 2010; MAFF, 2015), the total number of agricultural workers in the municipalities in Tokoro River Basin decreased by 15% (Table 4) from 2010 to 2015. The total area of agricultural fields also decreased, but this reduction was limited to 3%. Based on these data, it may be assumed that depopulation will be accompanied by a decrease in agricultural fields, although the reduction rate of agricultural fields will be lower than that of the population, because the study

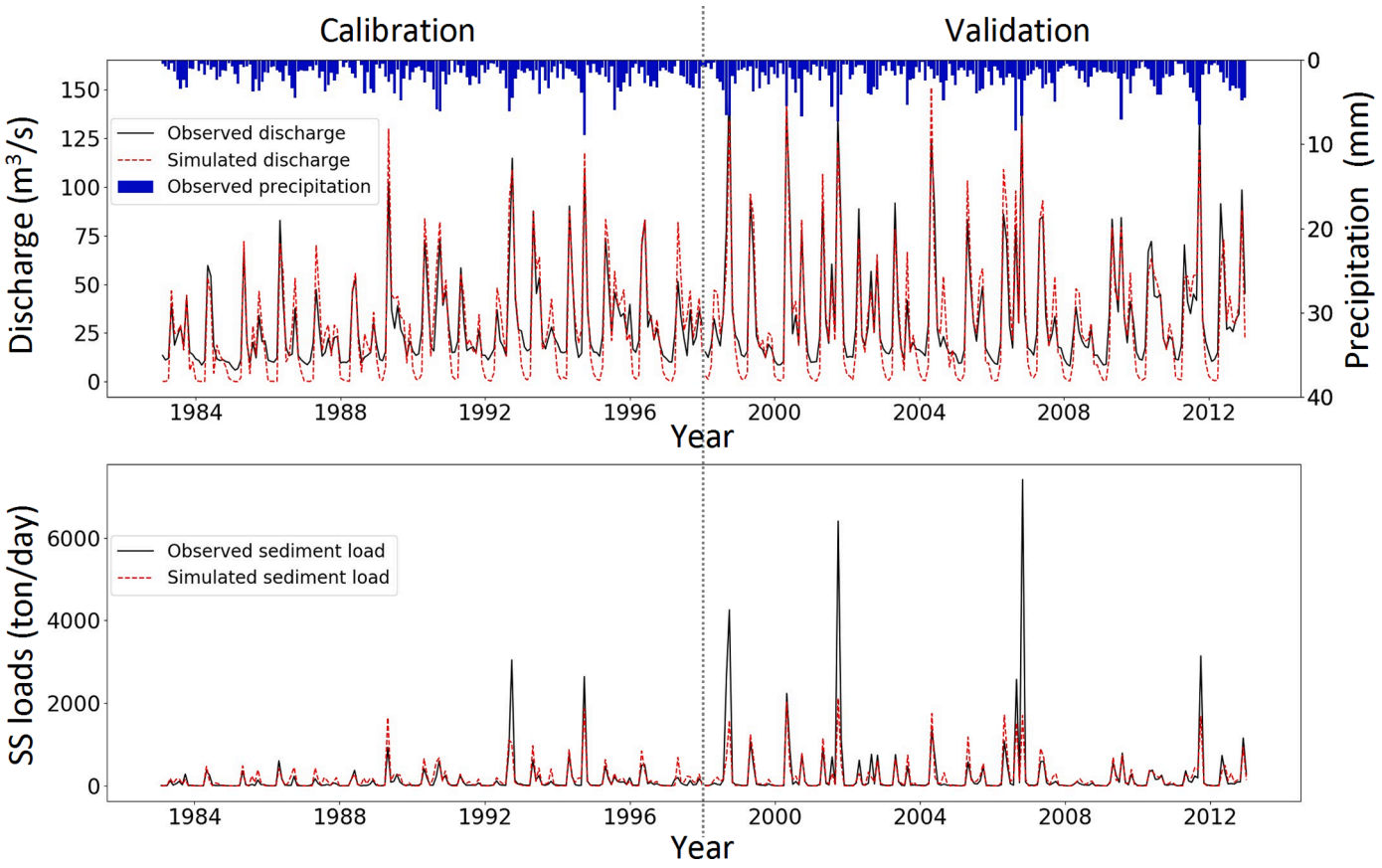

Fig. 5. Observed and simulated average daily discharge and suspended sediment (SS) loads at the Kamikawazoi hydrometric station, for the calibration and validation periods.

Table 5
Model performance regarding discharge and suspended sediment (SS) loads at the Kamikawazoi hydrometric station, for the calibration and validation periods. NSE - Nash-Sutcliffe efficiency; RSR - ratio of the root mean square error to the standard deviations; PBIAS - percent of bias.

	Calibration period			Validation period		
	NSE	RSR	PBIAS (%)	NSE	RSR	PBIAS (%)
Discharge	0.728	0.521	3.5	0.857	0.378	7.0
SS loads	0.642	0.598	22.3	0.517	0.695	24.9

Table 6
Average annual sediment yield (ton/ha) for each land-use type in the baseline, future climate, future land-use and combined future climate and land-use scenarios.

Land-use	Sediment yield (ton/ha)			
	Baseline	Future climate	Future land use	Future climate + future land use
Other agricultural land	6.5888	5.6926	-	-
Urban area	0.3125	0.2760	0.4544	0.4021
Forest	0.0009	0.0027	0.0026	0.0044
Rice paddy	-	-	4.1726	3.6095
Wasteland	-	-	0.1659	0.0612

area presents extensive plains that are suitable for the large-scale use of machinery. To consider a scenario with a significant impact, it was assumed that the reduction rate of agricultural fields due to depopulation in the future will be higher than the current trend.

New HRUs had to be created for the future land-use scenario. The thresholds of soil, slope, and land-use were set at 10%, and the number of HRUs for the future land-use scenario was 104.

3. Results and discussions

3.1. Model performance

Fig. 5 shows the simulated and observed average monthly discharge and SS loads at the Kamikawazoi hydrometric station. The model successfully simulated monthly discharge and SS loads according to the criteria referred by Moriasi et al. (2007).

The NSE and RSR values for discharge (Table 5) indicated good model performance for the calibration period (NSE = 0.728; RSR = 0.521) and very good model performance for the validation period (NSE = 0.857; RSR = 0.378). Moreover, the PBIAS for discharge was rated as very good (Moriasi et al., 2007) for the calibration (+3.5%) and validation (+7.0%) periods. Although these values were within the recommended ranges, positive PBIAS values are indicative of model underestimation. The underestimation of the model primarily occurred during low-flow seasons (i.e., winter) (Fig. 5), likely because SWAT does not consider the transfer of groundwater between different sub-basins (Neitsch et al., 2009).

In terms of SS loads, NSE and RSR values revealed satisfactory model performance for both the calibration (NSE = 0.642; RSR = 0.598) and validation (NSE = 0.517; RSR = 0.695) periods. The PBIAS values indicated good model performance for both the calibration (–22.3%) and validation (+24.9%) periods (Table 5). These findings point out that, although within the recommended ranges, the model overestimated the SS loads for the calibration period but underestimated them for the validation period. As shown in Fig. 5, there were a few remarkably high values in the observations for the validation period

Table 7
Average annual ET (mm) and PET (mm) for each land-use type in the baseline, future climate, future land-use and combined future climate and land-use scenarios.

Land-use	ET (mm) Baseline	Future climate	Future land use	Future climate + future land use	PET (mm) Baseline	Future climate	Future land use	Future climate + future land use
Other agricultural land	266.2	397.5	-	-	385.6	698.5	-	-
Urban area	282.1	422.3	278.6	423.7	398.0	707.5	398.0	707.5
Forest	230.9	355.8	232.4	358.4	366.2	675.0	367.5	675.8
Rice paddy	-	-	271.5	418.3	-	-	398.0	707.8
Wasteland	-	-	248.1	380.2	-	-	388.4	705.4

Table 8
Average annual suspended sediment (SS) loads, sediment yield and the ratio of SS loads by sediment yield in the baseline, future climate, future land-use and combined future climate and land-use scenarios.

	Baseline	Future climate	Future land use	Future climate + future land use
SS loads (10^6 kg/year)	71.4	65.0	72.7	46.9
Sediment yield (10^6 kg /year)	235.9	204.1	6.7	4.0
SS loads / Sediment yield	0.3	0.3	10.9	11.8

compared to the calibration period; thus explaining underestimation by the model.

3.2. Reproducibility of the baseline scenario

The results of the Mann-Whitney U tests (Table S1) revealed that there were no significant differences (p-value>0.05) between SWAT outputs using the JMA climate data and the observed discharge and SS loads (Fig. 6). The same was found when comparing SWAT results using the JMA climate data and in situ weather data (Fig. 6). These results indicate that the SWAT outputs using JMA historical climate data have successfully reproduced the observed discharge and SS loads. Thus, it is appropriate to use JMA historical climate data as the baseline climate scenario.

3.3. Future scenarios

3.3.1. Effects of climate change

Under the future climate scenario, the average annual discharge decreased by 23% compared to the baseline scenario (Fig. 7). This decrease appeared to be related to slight change in precipitation and a substantial increase in evapotranspiration (ET) (Fig. 8). Khoi and Suetsugi (2014) and Mango et al. (2011) also suggested that the ET has a large impact on discharge. Conversely, previous studies have referred that changes in precipitation exert a more significant effect on discharge than increases in ET (Hoque et al. 2014; Molina-Navarro et al., 2014; Shao et al., 2018).

The average monthly precipitation decreased in January, May, June, October, November and December, while it increased in March, April,

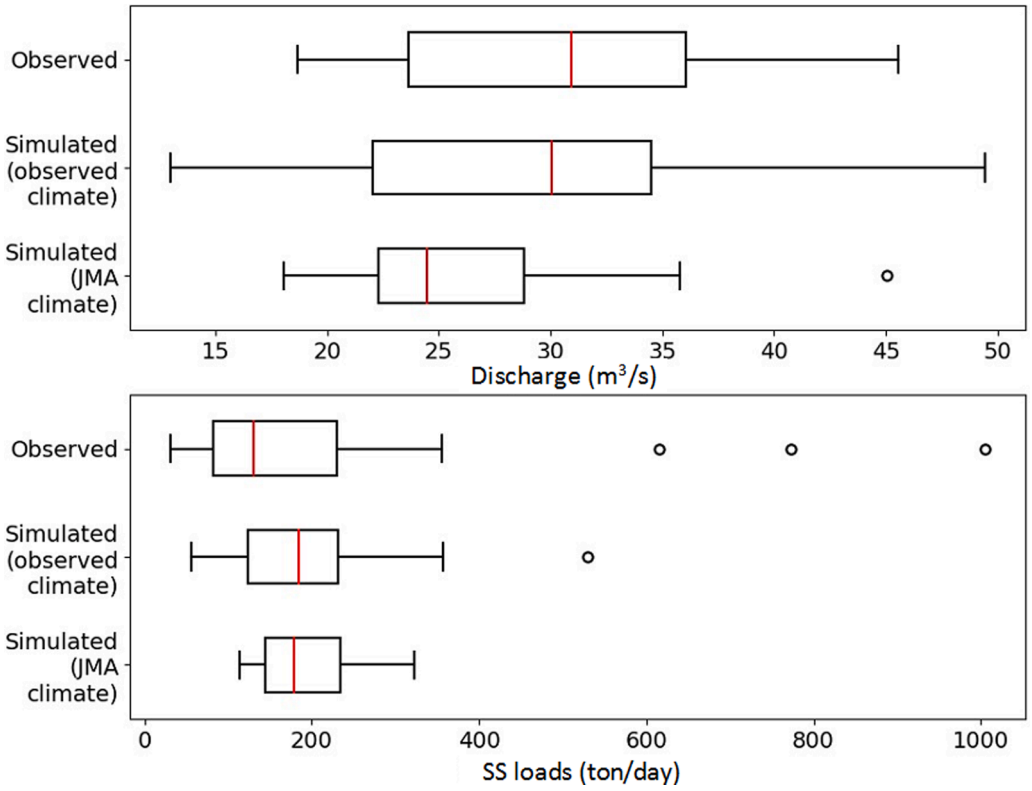

Fig. 6. Boxplots of the observed and simulated (using in situ weather data and JMA ensemble climate data) average annual discharge and suspended sediment (SS) loads. The red lines, boxes, whiskers, and white circles represent median values, the ranges from the 1st quartile to the 3rd quartile, the ranges of minimum and maximum values, and outliers, respectively. (For interpretation of the references to color in this figure legend, the reader is referred to the web version of this article.)

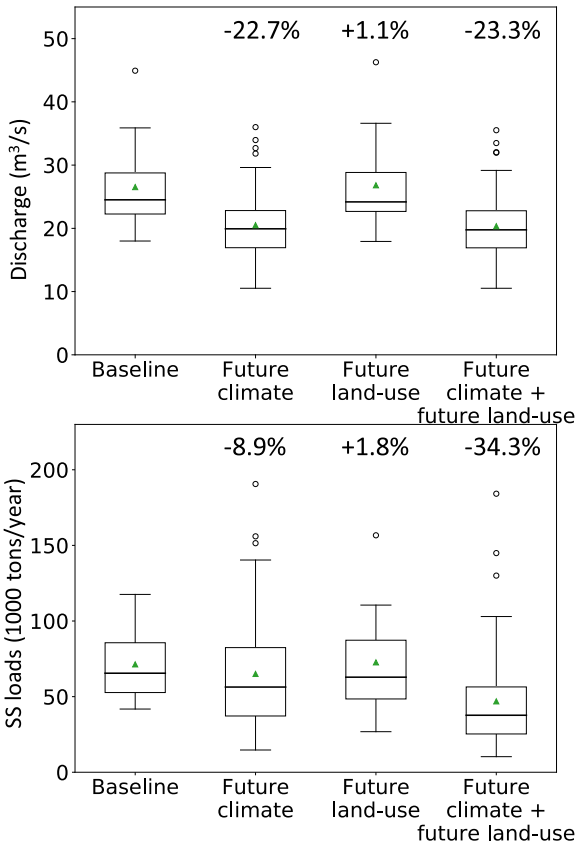

Fig. 7. Boxplots of the average annual discharge and SS loads for the baseline, future climate, future land-use and combined future climate and land-use scenarios. The lines inside the boxes, the boxes, the whiskers, and the white circles represent median values, the ranges from the 1st quartile to the 3rd quartile, the ranges of minimum and maximum values, and the outliers, respectively. The green triangles show the average values. The percentages written in the figures represent the relative change of the average values in each scenario compared to the baseline scenario. (For interpretation of the references to color in this figure legend, the reader is referred to the web version of this article.)

July, August and September (Fig. 9), though there was little change (+3%) in annual precipitation compared to the baseline scenario.

ET increased in every month except November, exhibiting an increase of more than 100% from January to May and December; which led annual ET to increase by 53% (Fig. 8). The increase in ET was assumed to have occurred due to a rise in temperature, as a similar increase was observed for monthly potential evapotranspiration (PET). The average temperature increased between 4.4 and 6.7°C every month (Fig. 8). Pervez and Henebry (2015) also indicated that temperature changes largely affected ET.

Average annual ET was higher in urban areas than in other land-use types regardless of climate change (Table 7). As a similar trend was observed in the average annual PET (Table 7), it was assumed that this ET increase in urban areas was due to higher temperatures. The urban areas are distributed in regions with relatively low elevations (Figs. 2 and 4); therefore, it is reasonable that the temperature in urban areas is relatively high.

Average annual SS loads decreased by 9% in the future climate scenario compared to the baseline scenario (Fig. 7). As the ratio between the average annual SS loads to sediment yield was 0.3 in both the baseline and future climate scenarios (Table 8), SS loads are related to sediment yield from the watershed in both scenarios. Therefore, the decrease in SS loads was assumed to have occurred due to a reduction in the sediment yield.

Average annual sediment yield in the watershed decreased by 13% in the future climate scenario (Table 8). The decrease in sediment yield in agricultural (–14%) and urban (–12%) areas had contributed to a generalized decrease in sediment yield under this scenario (Table 6). The reduction of sediment yield in agricultural and urban areas were assumed to have occurred because of a decrease in discharge.

In forests, the average annual sediment yield increased by 200% compared to the baseline scenario (Table 6), however this had little impact on the general change in sediment yield, since in forests, sediment yield was significantly lower than that of other land-use types. This increase was assumed to be related to a decrease in snowfall due to temperature rise (Fig. 9). The decrease (higher than 50%) in snowfall was particularly noticeable in April, October, November and December. Therefore, there is a possibility that sediment yield in forests increased because discharges derived from snowmelt were altered into discharges derived from rainfall as a result of the temperature increase. This hypothesis has also been referred in previous studies pertaining to snowfall regions (Kim et al., 2015; Somura et al., 2009).

3.3.2. *Effects of land-use change*

Under the future land-use scenario, there was little change (+1%) in the average annual discharge compared to the baseline scenario (Fig. 7). Although a large area of agricultural lands was converted into wastelands under the future land-use scenario, there were marginal differences between the annual ET from agricultural lands and wastelands in the baseline and future land use scenarios, respectively (Table 7). As such, land-use change almost did not exert any effect on discharge.

The average annual sediment yield in the watershed decreased by 97% in the future land-use scenario compared to the baseline scenario (Table 8). The main reason for this decrease was the conversion of a considerable area of agricultural lands into wastelands, since the latter have lower erodibility than the former (e.g., Olaniya et al., 2020). The average annual sediment yield per area was significantly smaller in the wastelands in the future land-use scenario (0.2 t/ha) than in the agricultural lands in the baseline scenario (6.6 t/ha) (Table 6). Previous studies have also indicated a decrease in sediment yield when agricultural lands are converted into grasslands or rangelands (Azimi Sardari et al., 2019; Calvaro-Santos et al., 2015; Hoque et al. 2014; Shao et al., 2018). Although the impact is small, the conversion of agricultural lands and urban areas to rice paddies also contributed to a decrease in the total sediment yield, since the erodibility of rice paddies was lower than that of agricultural lands and urban areas (Table 6).

The average annual sediment yield in urban areas and forests increased under the future land-use scenario (Table 6), but had little impact on the whole watershed, because the urban area occupies only a small area of the basin, and sediment yield from forests is considerably small compared to other land-use types. The increase in sediment yield in urban areas and forests appear to be related to the topography and soil type respectively. The ratio of urban areas that were located on steep land (i.e., slope >10%) was higher (65%) than that in the baseline scenario (49%). The ratio of forests that were located on soil types with relatively high erodibility (i.e., andosols and gray lowland soils) was also higher (3%) in the future land-use scenario than in the baseline scenario (0.6%).

Despite the decrease in sediment yield in the watershed, little change was observed in terms of the average annual SS loads in the future land-use scenario (+2%) compared to the baseline scenario (Fig. 7). This little change could be attributed to the following reasons. First, as the average annual discharge was similar in the baseline and future land-use scenarios, the sediment transport capacity was also similar. Second, the decrease in sediment yield from the watershed was complemented by channel erosion. The ratio between the average annual SS loads to sediment yield was 10.9 in the future land-use scenario (Table 8), which shows that, in this scenario, a substantial proportion of SS loads is provided by channel erosion instead of sediment yield from the watershed. As a consequence of the subtle change in discharge and a large decrease in sediment yield, land-use change shifted the main source of

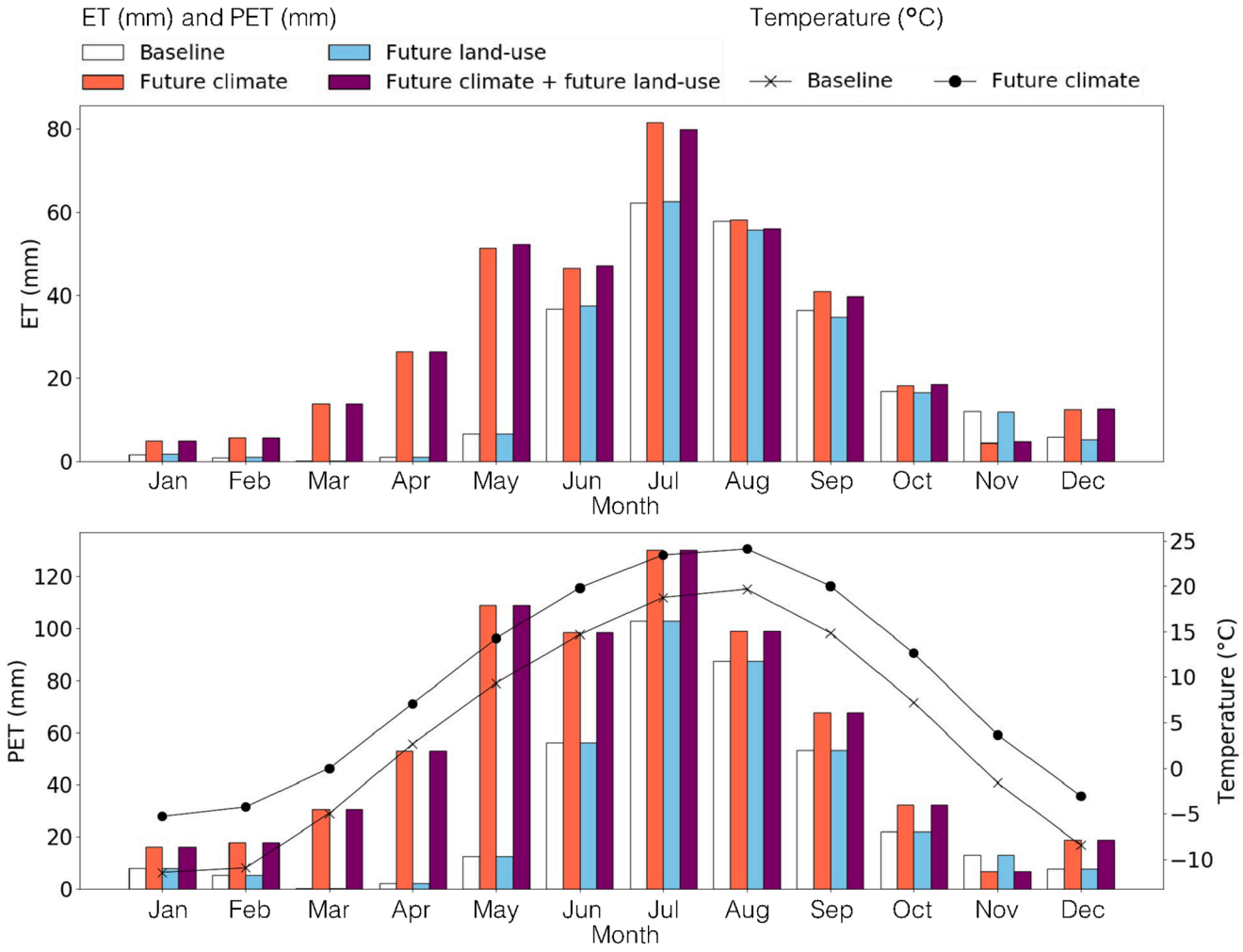

Fig. 8. Average monthly evapotranspiration (ET) and potential evapotranspiration (PET) under the baseline, future climate, future land-use and combined future climate and land-use scenarios; average monthly temperature for the baseline and future climate scenarios.

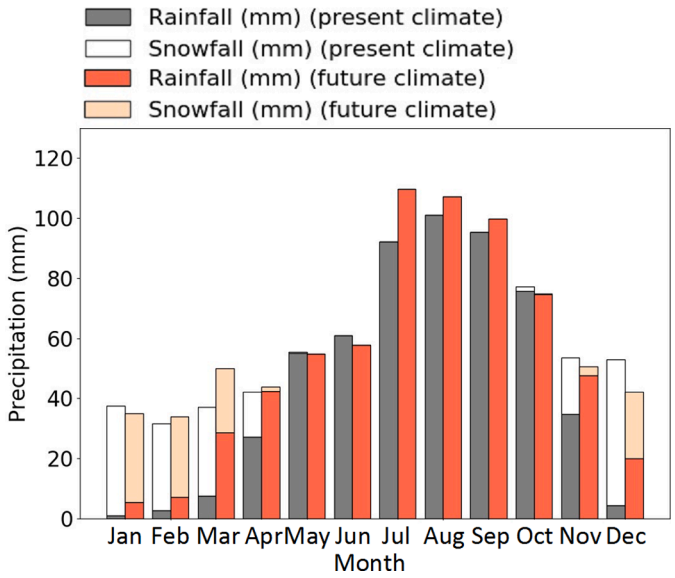

Fig. 9. Average monthly rainfall (mm) and snowfall (mm) under the baseline and future climate scenarios.

sediment supply from the watershed to channel erosion. These findings are consistent with those reported by Ishida et al. (2012), who analyzed the relationship between SS supplied from agricultural lands or forests and precipitation in a sub-basin of the Tokoro River Basin. According to the former authors, the SS concentrations derived from these two land types leveled off when precipitation exceeded a certain amount. Therefore, when the sediment transport capacity of the river is high, sediments are mostly provided by channel erosion. The results regarding sediment yield and channel erosion might be overestimated not only because the reduction in agricultural area is likely to be milder than what was considered in the future land-use scenario in this study, but also because the sediment supply by channel erosion will be limited when the bedrock of the river is exposed or armoring occurs, which has not been considered in this study.

Despite the possibility of overestimation, the results of this study indicated that the lack of land development due to depopulation may affect sediment regimes in river basins by accelerating channel erosion. These findings provide additional perspectives to the work of Nakamura et al. (2017), which have indicated that active land developments such as dam construction or gravel mining have affected sediment regimes in some Japanese rivers basins.

3.3.3. *Combined effects of climate and land-use change*

Under the combined future climate and land-use change scenario, the average annual discharge decreased by 23% compared to the baseline scenario (Fig. 7). This decrease is similar to the decrease under the

future climate scenario, suggesting that the magnitude of the impacts of climate change on discharge is independent from land-use.

Similar to the future climate scenario, it was assumed that the increase in ET was the primary cause of discharge decrease under the combined future climate and land-use change scenario. As noted in case of the future climate scenario, ET and PET increased every month, and the annual ET increased by 52% (Fig. 8).

The average annual SS loads decreased by 34% compared to the baseline scenario. The decrease in SS loads under the combined scenario was larger than the decrease under the individual climate scenario. This appears to be related to a decrease in both discharge and sediment yield. As both climate and land-use changes lead to decreases in sediment yield, the reduction is the largest when the impacts from both changes are combined. Additionally, the average annual discharge decreased in the combined scenario, which led to a small channel erosion rate, and in turn to a significant decrease in SS loads under this scenario.

The ratio of average annual SS loads to sediment yield in the combined scenario was similar to that in the individual land-use scenario (Table 8). These results indicate that a substantial proportion of SS loads is derived from channel erosion in both the combined and individual land-use scenarios. Despite the different changes in SS loads between the combined and independent future land-use scenarios, similar changes in sediment regimes (i.e., the acceleration of channel erosion) occurred.

Despite evaluating the combined effects of climate and land-use changes, this work assumed that these changes occurred independently. However, in reality, there will likely be interactions between climate and land-use changes. For example, Piao et al. (2003) have indicated that an increase in temperature contributes to increased vegetation growth. If similar trends are observed in this study area and if the productivity of agricultural lands increases, there is a possibility that the area of these lands will not be reduced to the extent predicted in this study. Therefore, it is possible that the foreseen decrease in sediment yield when combing land-use and climate changes is overestimated.

4. Conclusions

This study examined the separate and combined impacts of climate and land-use changes on water and sediment dynamics for a river basin in northern Japan. The results of this study highlighted the dominating impact of climate change on discharge as well as the possibility of transition in sediment regimes (i.e., transition of the source of sediment supply from watershed to channels) due to depopulation. This study provides an important perspective for future river management.

Although the methodology followed in this study was reasonable for achieving the aims of this study, some uncertainties remain:

(1) Uncertainties related to the observed data– as the SS concentrations were measured only once or twice a month, these observations might not fully reflect the impacts of flood events. Moreover, as the observed SS loads were interpolated to fulfill data gaps, they might not fully reflect the reality of the basin. Thus, there is a possibility that the change in SS loads resulting from changes in flood regimes under climate change might not have been completely captured, so monitoring at a higher frequency is recommended for this basin.
(2) Model uncertainties– as the SWAT model does not consider the transfer of groundwater between different sub-basins, the model results might not fully reflect the difference in discharge during low-flow seasons.
(3) Climate scenario uncertainties– as the future climate scenario was simulated by a single GCM, multiple patterns of climate variability may not have been accounted in this study, even if four different sea surface warming patterns were considered. Moreover, as only the worst-case scenario of greenhouse gas emissions, i.e., RCP 8.5, was analyzed, smaller decreases in discharge and SS loads are expected under milder scenarios of greenhouse gas emissions (e.g., RCP 4.5 or 6.0).
(4) Land-use scenario uncertainties– as this study considers an extreme scenario of reduction in agricultural areas due to depopulation, the reduction in sediment yield might be overestimated, so caution should be taken when using the results of the present study.

Despite the associated uncertainties, this work advanced the current knowledge on the impacts of climate and land-use changes in water and sediment dynamics in a river basin facing depopulation. The results emphasized the importance of understanding the combined effects of climate and land-use changes to better manage land and water resources. The results will offer essential information for areas in which depopulation is currently occurring or is forecasted to occur.

CRediT authorship contribution statement

Yuka Muto: Conceptualization, Methodology, Formal analysis, Writing – original draft. **Keigo Noda:** Methodology, Writing – review & editing. **Yasuyuki Maruya:** Resources, Writing – review & editing. **Takeyoshi Chibana:** Supervision, Writing – review & editing. **Satoshi Watanabe:** Conceptualization, Methodology, Resources, Supervision, Writing – review & editing.

Declaration of Competing Interest

The authors declare that they have no known competing financial interests or personal relationships that could have appeared to influence the work reported in this paper.

Acknowledgments

This study was supported by the Grants in Aid for Scientific Research (Nos. 21J11113, 18K13834 and 21H05178) from the Japan Society for the Promotion of Science (JSPS), the River Fund (2021-5311-004) from the River Foundation, and the Program for Integrated Research Program for Advancing Climate Models (JPMXD0717935498) from the Ministry of Education, Culture, Sports, Science, and Technology, Japan (MEXT). The dataset of JMA-GWP9 was produced under the SOUSEI and TOUGOU programs. We would like to thank Editage (www.editage.com) for English language editing.

Supplementary materials

Supplementary material associated with this article can be found, in the online version, at doi:10.1016/j.envadv.2021.100153.

References

Abbaspour, K.C., 2015. SWAT-CUP: SWAT Calibration and Uncertainty Programs -A User Manual. Swiss Federal Institute of Aquatic Science and Technology, pp. 1–100. Eawag, Dübendorf.

Azimi Sardari, M.R.A., Bazrafshan, O., Panagopoulos, T., Sardooi, E.R., 2019. Modeling the impact of climate change and land use change scenarios on soil erosion at the Minab Dam watershed. Sustainability 11 (3353), 3353. https://doi.org/10.3390/su11123353 doi:

Bagnold, R.A., 1977. Bedload transport in natural rivers. Water Resour. Res. 13, 303–312. https://doi.org/10.1029/WR013i002p00303.

Beguería, S., López-Moreno, J.I., Lorente, A., Seeger, M., García-Ruiz, J.M., 2003. Assessing the effect of climate oscillations and land-use changes on streamflow in the central Spanish Pyrenees. AMBIO J. Hum. Environ. 32, 283–286. https://doi.org/10.1579/0044-7447-32.4.283.

Carvalho-Santos, C., Nunes, J.P., Monteiro, A.T., Hein, L., Honrado, J.P., 2015. Assessing the effects of land cover and future climate conditions on the provision of hydrological services in a medium-sized watershed of Portugal. Hydrol. Process. 30, 720–738. https://doi.org/10.1002/hyp.10621.

GIAJ, Geospatial information authority of Japan 2021 fundamental geospatial data digital elevation mesh 10m mesh. (https://fgd.gsi.go.jp/download/menu.php) (in Japanese) (Last accessed in May 2021).

Gupta, H.V., Sorooshian, S., Yapo, P.O., 1999. Status of automatic calibration for hydrologic models: comparison with multilevel expert calibration. J. Hydrol. Eng. 4, 135–143.
Hoque, Y.M., Raj, C., Hantush, M., Chaubey, I., Govindaraju, R.S., 2014. How do land-use and climate change affect watershed health? A scenario-based analysis. Water Qual. Expo. Health 6, 19–33. https://doi.org/10.1007/s12403-013-0102-6.
Ishida, T., Nakayama, K., Okada, T., Maruya, Y., Onishi, K., Omori, M., 2010. Suspended sediment transport in a river basin estimated by chemical composition analysis. Hydrol. Res. Lett. 4, 55–59. https://doi.org/10.3178/HRL.4.55.
Ishida, T., Hayakawa, H., Nakayama, K., Okada, T., Maruya, Y., Komai, K., Hotta, N., Fujii, Kato, J., 2012. Evaluation of suspended sediment transport in a river basin by using chemical composition analysis. J. Jpn. Soc. Civ. Eng. B1 (Hydraul. Eng.) 68 (4), 637–642. https://doi.org/10.2208/jscejhe.68.I_637 (in Japanese).
JMA, Japan Meteorological Agency, 2017. Japan Meteorological Agency Global Warming Projection Volume 9. JMA, pp. 1–26 (in Japanese).
Kalantari, Z., Lyon, S.W., Folkeson, L., French, H.K., Stolte, J., Jansson, P.E., Sassner, M., 2014. Quantifying the hydrological impact of simulated changes in land use on peak discharge in a small catchment. Sci. Total Environ. 466–467, 741–754. https://doi.org/10.1016/j.scitotenv.2013.07.047.
Kalogeropoulos, K., Chalkias, C., 2013. Modelling the impacts of climate change on surface runoff in small Mediterranean catchments: empirical evidence from Greece. Water Environ. J. 27, 505–513. https://doi.org/10.1111/j.1747-6593.2012.00369.x.
Khoi, D.N., Suetsugi, T., 2014. The responses of hydrological processes and sediment yield to land-use and climate change in the Be River Catchment, Vietnam. Hydrol. Process. 28, 640–652. https://doi.org/10.1002/hyp.9620.
Khoi, D.N., Thom, V.T., 2015. Parameter uncertainty analysis for simulating streamflow in a river catchment of Vietnam. Glob. Ecol. Conserv. 4, 538–548. https://doi.org/10.1016/j.gecco.2015.10.007 doi:
Khoi, D.N., Thom, V.T., Quang, C.N.X., Phi, H.L., et al., 2017. Parameter Uncertainty Analysis for Simulating Streamflow in the Upper Dong Nai River Basin 103, 14–23. La Houille Blanche.
Kim, S.B., Shin, H.J., Park, M., Kim, S.J., 2015. Assessment of future climate change impacts on snowmelt and stream water quality for a mountainous high-elevation watershed using SWAT. Paddy Water Environ. 13, 557–569. https://doi.org/10.1007/s10333-014-0471-x.
Kitami city 2020 The vision of the population in Kitami City. (https://www.city.kitami.lg.jp/common/img/content/content_20210330_152135.pdf) (in Japanese) (Last accessed in July 2021).
Kunneppu city 2020 The vision and the total strategy of population: revitalizing the city, people and jobs in Kunnneppu City, Period 2. (https://www.town.kunneppu.hokkaido.jp/fs/5/5/7/9/_/20kisougou.pdf) (in Japanese) (Last accessed in July 2021).
Li, H., Zhang, Y., Vaze, J., Wang, B., 2012. Separating effects of vegetation change and climate variability using hydrological modelling and sensitivity-based approaches. J. Hydrol. 420–421, 403–418. https://doi.org/10.1016/j.jhydrol.2011.12.033.
Li, Z., Liu, W.Z., Zhang, X.C., Zheng, F.L., 2009. Impacts of land use change and climate variability on hydrology in an agricultural catchment on the Loess Plateau of China. J. Hydrol. 377, 35–42. https://doi.org/10.1016/j.jhydrol.2009.08.007.
Local committee of clean stream renaissance in the Tokoro River basin 2009 Urgent plans for improving the water environment in the Tokoro River Basin. (https://www.hkd.mlit.go.jp/ab/tisui/v6dkjr0000000ao0-att/v6dkjr0000000ara.pdf) (in Japanese) (Last accessed in July 2021).
López-Moreno, J.I., Zabalza, J., Vicente-Serrano, S.M., Revuelto, J., Gilaberte, M., Azorin-Molina, C., Morán-Tejeda, E., García-Ruiz, J.M., Tague, C., 2014. Impact of climate and land use change on water availability and reservoir management: scenarios in the Upper Aragón River, Spanish Pyrenees. Sci. Total Environ. 493, 1222–1231.
Luo, Y., Ficklin, D.L., Liu, X., Zhang, M., 2013. Assessment of climate change impacts on hydrology and water quality with a watershed modeling approach. Sci. Total Environ. 450–451, 72–82. https://doi.org/10.1016/j.scitotenv.2013.02.004.
MAFF, Ministry of Agriculture, Forestry and Fisheries 2010 2010 world census of agriculture and forestry in Japan. (https://www.e-stat.go.jp/stat-search/files?page=1&layout=datalist&toukei=00500209&tstat=000001032920&cycle=0&tclass1=000001038546&tclass2=000001045941&tclass3=000001047444&tclass4=000001047445) (in Japanese) (Last accessed in May 2021).
MAFF, Ministry of Agriculture, Forestry and Fisheries 2015 2015 census of agriculture and forestry in Japan. (https://www.e-stat.go.jp/stat-search/files?page=1&layout=datalist&toukei=00500209&tstat=000001032920&cycle=0&tclass1=0000010 77437&tclass2=000001077396&tclass3=000001093235&tclass4=000001093236) (in Japanese) (Last accessed in May 2021).
Mango, L.M., Melesse, A.M., McClain, M.E., Gann D and Setegn, S.G., 2011. Land use and climate change impacts on the hydrology of the upper Mara River Basin, Kenya: results of a modeling study to support better resource management. Hydrol. Earth Syst. Sci. 15, 2245–2258. https://doi.org/10.5194/hess-15-2245-2011.
Mann, H.B., Whitney, D.R., 1947. On a test of whether one of two random variables is stochastically larger than the other. Ann. Math. Stat. 18, 50–60. https://doi.org/10.1214/aoms/1177730491.
MECSST and JMA, Ministry of Education, Culture, Sports, Science and Technology and Japan Meteorological Agency 2020 Climate change in Japan 2020—a report on the evaluations of observations and predictions related to atmosphere, land and ocean—. (https://www.data.jma.go.jp/cpdinfo/ccj/2020/pdf/cc2020_honpen.pdf) (in Japanese) (Last accessed in December 2021).
Meng, F., Su, F., Yang, D., Tong, K., Hao, Z., 2016. Impacts of recent climate change on the hydrology in the source region of the Yellow River basin. J. Hydrol. Reg. Stud. 6, 66–81. https://doi.org/10.1016/j.ejrh.2016.03.003.
Milly, P.C.D., Dunne, K.A., Vecchia, A.V., 2005. Global pattern of trends in streamflow and water availability in a changing climate. Nature 438, 347–350. https://doi.org/10.1038/nature04312.
Mizuta, R., Yoshimura, H., Murakami, H., Matsueda, M., Endo, H., Ose, T., Kamiguchi, K., Hosaka, M., Sugi, M., Yukimoto, S., Kusunoki, S., Kitoh, A., 2012. Climate simulations using MRI-AGCM3.2 with 20-km grid. J. Meteorol. Soc. Jpn. 90A, 233–258. https://doi.org/10.2151/jmsj.2012-A12.
MLIT, Ministry of Land, Infrastructure, Transport and Tourism 2021a Digital National Land Information: river data. (https://nlftp.mlit.go.jp/ksj/jpgis/datalist/KsjTmplt-W05.html) (in Japanese) (Last accessed in May 2021).
MLIT, Ministry of Land, Infrastructure, Transport and Tourism 2021b Japan water information system. (http://www1.river.go.jp/) (in Japanese) (Last accessed in May 2021).
MLIT, Ministry of Land, Infrastructure, Transport and Tourism 2021c 2009 subdivision mesh data Digital National Land Information: Japan land use. (https://nlftp.mlit.go.jp/ksj/gml/datalist/KsjTmplt-L03-b.html) (in Japanese) (Last accessed in May 2021).
MLIT, Ministry of Land, Infrastructure, Transport and Tourism 2009 Methods for measuring water quality in rivers. (https://www.mlit.go.jp/river/shishin_guideline/kasen/suishitsu/pdf/s04.pdf) (in Japanese) (Last accessed in July 2021).
MLIT, Ministry of Land, Infrastructure, Transport and Tourism, Japan 2006 The overview information of the catchment and rivers of the Tokoro Water System (draft). (https://www.mlit.go.jp/river/shinngikai_blog/shaseishin/kasenbunkakai/shouiinkai/kihonhoushin/061031/pdf/ref1-1.pdf) (in Japanese) (Last accessed in May 2021).
Molina-Navarro, E., Trolle, D., Martínez-Pérez, S., Sastre-Merlín, A., Jeppesen, E., 2014. Hydrological and water quality impact assessment of a Mediterranean limno-reservoir under climate change and land use management scenarios. J. Hydrol. 509, 354–366. https://doi.org/10.1016/j.jhydrol.2013.11.053.
Montenegro, S., Ragab, R., 2012. Impact of possible climate and land use changes in the semi arid regions: a case study from North Eastern Brazil. J. Hydrol. 434–435, 55–68. https://doi.org/10.1016/j.jhydrol.2012.02.036.
Moriasi, D.N., Arnold, J.G., Van Liew, M.W., Bingner, R.L., Harmel, R.D., Veith, T.L., 2007. Model evaluation guidelines for systematic quantification of accuracy in watershed simulations. Trans. ASABE 50, 885–900. https://doi.org/10.13031/2013.23153.
Mourato, S., Moreira, M., Corte-Real, J., 2015. Water resources impact assessment under climate change scenarios in Mediterranean watersheds. Water Resour. Manag. 29, 2377–2391. https://doi.org/10.1007/S11269-015-0947-5.
Nakamura, F., Seo, J.I., Akasaka, T., Swanson, F.J., 2017. Large wood, sediment, and flow regimes: Their interactions and temporal changes caused by human impacts in Japan. Geomorphology 279, 176–187. https://doi.org/10.1016/j.geomorph.2016.09.001.
Nash, J.E., Sutcliffe, J.V., 1970. River flow forecasting through conceptual models part I — a discussion of principles. J. Hydrol. 10, 282–290. https://doi.org/10.1016/0022-1694(70)90255-6.
NIPSSP, National Institute of Population and Social Security Research 2018 Regional population projections for Japan: 2015–2045. Population research series 340 (in Japanese).
Neitsch, S.L., Arnold, J.G., Kiniry, J.R., Williams, J.R., 2009. Soil and Water Assessment Tool Theoretical Documentation Version 2009. Texas Water Resources Institute, College Station, Texas, USA.
Noda, K., Iida, A., Watanabe, S., Osawa, K., 2019. Efficiency and sustainability of land-resource use on a small island. Environ. Res. Lett. 14, 054004 https://doi.org/10.1088/1748-9326/ab1455.
Noda, K., Yoshida, K., Shirakawa, H., Surahman, U., Oki, K., 2017. Effect of land use change driven by economic growth on sedimentation in river reach in Southeast Asia: –a case study in upper Citarum River Basin–. J. Agric. Meteorol. 73, 22–30. https://doi.org/10.2480/agrmet.D-15-00021.
Olaniya, M., Bora, K.P., Das, S., Chanu, H.P., 2020. Soil erodibility indices under different land uses in Ri-Bhoi district of Meghalaya (India). Sci. Rep. 10 https://doi.org/10.1038/s41598-020-72070-y.
Pervez, M.S., Henebry, G.M., 2015. Assessing the impacts of climate and land use and land cover change on the freshwater availability in the Brahmaputra River basin. J. Hydrol. Reg. Stud. 3, 285–311. https://doi.org/10.1016/j.ejrh.2014.09.003.
Piao, S., Fang, J., Zhou, L., Guo, Q., Henderson, M., Ji, W., Li, Y., Tao, S., 2003. Interannual variations of monthly and seasonal normalized difference vegetation index (NDVI) in China from 1982 to 1999. J. Geophys. Res. 108 https://doi.org/10.1029/2002JD002848.
Pinokius, M., Varanou, E., Baltas, E., Dassaklis, A., Mimikou, M., 2003. Application of the SWAT model in the Pinios river basin under different land-use scenarios. Glob. NEST Int. J. 5, 71–79.
Sasaki, H., Murata, A., Hanafusa, M., Oh'izumi, M., Kurihara, K., 2011. Reproducibility of present climate in a non-hydrostatic regional climate model nested within an atmosphere general circulation model. SOLA 7, 173–176. https://doi.org/10.2151/sola.2011-044.
SB and MIAC, Statistics Bureau and Ministry of Internal affairs and Communications 2021 Population census 1925. (https://www.e-stat.go.jp/en/stat-search/files?page=1&layout=datalist&toukei=00200521&tstat=000001036874&cycle=0&tclass1=000001037043&tclass2val=0) (Last accessed in May 2021).
SCS, Soil Conservation Service, 1985. National Engineering Handbook, Section 4 Hydrology. Soil Conservation Service, USDA, Washington District of Columbia.
Serpa, D., Nunes, J.P., Santos, J., Sampaio, E., Jacinto, R., Veiga, S., Lima, J.C., Moreira, M., Corte-Real, J., Keizer, J., Abrantes, N., 2015. Impacts of climate and land use changes on the hydrological and erosion processes of two contrasting Mediterranean catchments. Sci. Total Environ. 538, 64–77. https://doi.org/10.1016/j.scitotenv.2015.08.033.

Shao, G., Guan, Y., Zhang, D., Yu, B., Zhu, J., 2018. The impacts of climate variability and land use change on streamflow in the Hailiutu River Basin. Water 10 (814), 814. https://doi.org/10.3390/w10060814.

Singh, J., Knapp, H.V., Demissie, M., 2004. Hydrologic modeling of the Iroquois River watershed using HSPF and SWAT. Illinois State Water Survey, pp. 1–24.

Somura, H., Arnold, J., Hoffman, D., Takeda, I., Mori, Y., Di Luzio, M.D., 2009. Impact of climate change on the Hii River Basin and salinity in Lake Shinji: a case study using the SWAT model and a regression curve. Hydrol. Process. 23, 1887–1900. https://doi.org/10.1002/hyp.7321.

Tuo, Y., Marcolini, G., Disse, M., Chiogna, G., 2018. Calibration of snow parameters in SWAT: Comparison of three approaches in the Upper Adige River basin (Italy). Hydrol. Sci. J. 63, 657–678. https://doi.org/10.1080/02626667.2018.1439172.

Walling, D.E., 2006. Human impact on land–ocean sediment transfer by the world's rivers. Geomorphology 79, 192–216. https://doi.org/10.1016/j.geomorph.2006.06.019.

Watanabe, S., Yamada, M., Abe, S., Hatono, M., 2020. Bias correction of d4PDF using a moving window method and their uncertainty analysis in estimation and projection of design rainfall depth. Hydrol. Res. Lett. 14 (3), 117–122. https://doi.org/10.3178/hrl.14.117.

Watson, D.F., Philip, G.M., 1985. A refinement of inverse distance weighted interpolation. Geoprocessing 2 (4), 315–327.

Williams, J.R., 1975. Sediment routing for agricultural watersheds. J. Am. Water Resour. Assoc. 11, 965–974. https://doi.org/10.1111/j.1752-1688.1975.tb01817.x.

Wilson, C.O., Weng, Q., 2011. Simulating the impacts of future land use and climate changes on surface water quality in the Des Plaines River watershed, Chicago metropolitan statistical area, Illinois. Sci. Total Environ. 409, 4387–4405. https://doi.org/10.1016/j.scitotenv.2011.07.001.

Zabaleta, A., Meaurio, M., Ruiz, E., Antigüedad, I.A., 2014. Simulation climate change impact on runoff and sediment yield in a small watershed in the Basque country, Northern Spain. J. Environ. Qual. 43, 235–245. https://doi.org/10.2134/jeq2012.0209.

Zhang, A., Zhang, C., Fu, G., Wang, B., Bao, Z., Zheng, H., 2012. Assessments of impacts of climate change and human activities on runoff with SWAT for the Huifa River Basin, Northeast China. Water Resour. Manag. 26, 2199–2217. https://doi.org/10.1007/s11269-012-0010-8.